SMGroup

SM Journal of Food and Nutritional Disorders

Research Article

Transformation of the Physico-Chemical, Thermal, and Behavioral Properties of Tetrahydrocurcumin by means of the Consciousness Energy Healing Treatment

Mahendra Kumar Trivedi[1] and Snehasis Jana[2*]

[1]*Trivedi Global, Inc., USA*

[2]*Trivedi Science Research Laboratory Pvt. Ltd., India*

Article Information

Received date: Aug 30, 2019
Accepted date: Nov 01, 2019
Published date: Nov 04, 2019

***Corresponding author**

Snehasis Jana, Trivedi Science Research Laboratory Pvt. Ltd., Thane (W), Maharashtra, India

Tel: +91- 022-25811234

Email: publication@trivedieffect.com

Keywords Tetrahydrocurcumin; The Trivedi Effect®; Biofield energy; Consciousness energy healing treatment; PXRD; Particle size; DSC; TGA/DTG

Abstract

Tetrahydrocurcumin (THC) is a major metabolite of curcumin used as an antioxidant, anti-inflammatory, antiarthritic, anticancer, etc. The objective of this study was to evaluate the impact of the Trivedi Effect® - Biofield Energy Healing Treatment on the physicochemical, thermal, and behavioral properties of THC using sophisticated analytical techniques. The test sample was divided into two parts, one part of THC was considered as a control sample, while another part received the Biofield Energy Healing Treatment remotely by a famous Biofield Energy Healer, Mr. Mahendra Kumar Trivedi. The PXRD data showed that the THC was crystalline in nature. The relative peak intensities and crystallite sizes of the Biofield Energy Treated sample were significantly altered ranging from -17.76% to 17.20% and -26.68% to 326.39%, respectively compared to the control sample. However, the average crystallite size of the treated THC was decreased by 2.50% compared with the control sample. The particle size values of the treated sample were significantly decreased by 11.58% (d_{10}), 14.41% (d_{50}), 15.53% (d_{90}), and 15.23% {D(4,3)} compared with the control sample. Thus, the surface area of the treated sample was significantly increased by 14.24% compared with the control sample. The melting point and latent heat of fusion were decreased by 0.40% and 0.70%, respectively, in the treated sample compared to the control sample. The weight loss and maximum thermal degradation temperature in the treated THC were decreased by 0.62% and 1.54%, respectively compared with the control sample. Overall, the thermal analysis indicated that the thermal stability of the Biofield Energy Treated THC was declined compared to the control sample. The Trivedi Effect® -Consciousness Energy Healing Treatment might lead to the production of a new polymorphic form of THC, which would be more soluble and bioavailable compared with the untreated THC. The Treated THC would be very useful to design more efficacious nutraceutical/pharmaceutical formulations against the inflammatory diseases, arthritis, cancer, diabetes, hepatotoxicity, nephrotoxicity, etc.

Introduction

Tetrahydrocurcumin (THC) is a colorless or white polyphenolic metabolite of curcumin and quite similar physiological and pharmacological properties of curcumin [1,2]. In contrast, THC showed the strongest antioxidant activity than the other naturally-occurring curcuminoids, including curcumin, demethoxycurcumin, and bisdemethoxycurcumin [2-5]. It has different molecular targets, signaling pathways, cellular responses, and clinically more advantageous compared with the curcumin [2-5]. Many studies reported that THC has significant results in preventing inflammation, hepatotoxicity, nephrotoxicity, cancer, diabetes, rheumatoid arthritis, the ageing process, atherosclerotic lesions treatment, etc. [2-7]. However, THC does not have toxicity even at higher doses and can be used against tumors of the skin, colon, pancreas, breast, and other skin diseases like psoriasis, and scleroderma. [5,7]. THC plays a notable role in angiogenesis and also improves the accumulation of extracellular matrix (ECM) components through the remodeling of the wound repair [5].

The chemical structure of the THC is found in two different forms, such as diketo and keto-enol tautomeric form (Figure 1) [8]. The degradation half-lives of THC is 813 minutes in cell culture medium and 232 min in plasma [2]. However, many studies conducted on the bioavailability of THC and was found better bioavailable in the intestine, hepatic cytosol, brain, *etc.* compared to the curcumin but neither THC nor curcumin was detected in the plasma of mice [9]. Better bioavailability in the animal body is the major issue for THC. The Biofield Energy Treatment (the Trivedi Effect®) could be an economical approach for the reduction of particle size and improvement of the surface area; hence the bioavailability of THC can be increased [10,11].

The human body can discharge the electromagnetic waves in the form of bio-photons that surrounds the body. This electromagnetic energy is generated by the continuous movement of the electrically charged particles (ions, cells, etc.) inside the body. This energy is collectively known as "Biofield Energy". Biofield Energy Healing practitioners have the ability to harness the energy from the "Universal Energy Field" and can transmit into any living or non-living object(s) around the earth. The process, where the objects receive the Biofield Energy Treatment and respond into

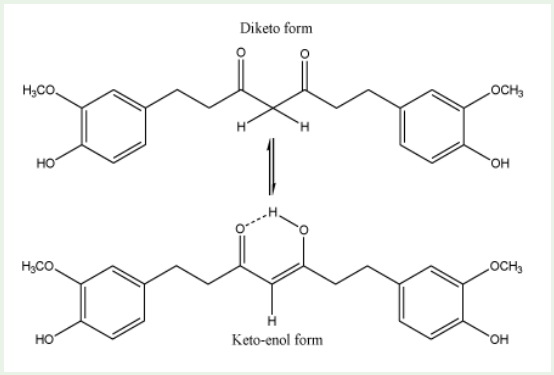

Figure 1: Structure of tetrahydrocurcumin with diketo and keto-enol resonance form.

a useful way, is called as Biofield Energy Healing [12-14]. Biofield based Energy Therapies are used worldwide to promote health and healing. The National Center of Complementary and Integrative Health (NCCIH) has recognized and accepted Biofield Energy Healing as a Complementary and Alternative Medicine (CAM) health care approach in addition to other therapies, medicines and practices such as natural products, deep breathing, yoga, Qi Gong, Tai Chi, chiropractic/osteopathic manipulation, meditation, special diets, massage, homeopathy, progressive relaxation, guided imagery, acupressure, acupuncture, relaxation techniques, healing touch, hypnotherapy, movement therapy, rolfing structural integration, pilates, mindfulness, naturopathy, Ayurvedic medicine, traditional Chinese herbs and medicines, aromatherapy, essential oils, Reiki, cranial-sacral therapy and applied prayer (as is common in all religions, like Hinduism, Christianity, Buddhism and Judaism) [15]. The Biofield Energy Healing Treatment had been expansively reported with significant results in different scientific fields like materials science [10,11,16-19], agricultural science [20-22], cancer research [23,24], microbiology [25-28], genetics [29,30], pharmaceutical science [31-34], etc.

The physicochemical properties such as crystalline structure, crystallite size, particle size, surface area, etc. of a drug play an important role in bioavailability, as these factors have the direct influence on solubility, absorption, and stability of the drug [35]. The particle size, specific surface area, crystalline nature, chemical and thermal behaviour of an atom/ion might be altered by the Trivedi Effect® through the possible mediation of neutrinos [36]. Thus, this study has been designed to evaluate the impact of the Trivedi Effect®-Consciousness Energy Healing Treatment on the physicochemical, thermal, structural, and behavioral properties of tetrahydrocurcumin using sophisticated analytical techniques.

Materials and Methods

Chemicals and Reagents

The test sample tetrahydrocurcumin 95% was purchased from Novel Nutrients Pvt. Ltd., and other chemicals used in the experiments were purchased in India.

Consciousness energy healing treatment strategies

The test sample tetrahydrocurcumin was divided into two parts. One part of THC was considered as control, where no biofield treatment was provided; while the second part of THC was received the Trivedi Effect®-Consciousness Energy Healing Treatment remotely under standard laboratory conditions for 3 minutes by a famous Biofield Energy Healer, Mr. Mahendra Kumar Trivedi and known as Biofield Energy Treated sample. Further, the control THC was treated with a "sham" healer, who did not have any knowledge about the Biofield Energy Treatment. After that, both the samples were kept in sealed conditions and characterized using sophisticated analytical techniques.

Characterization

The powder X-ray diffraction (PXRD) analysis of THC powder sample was performed with the help of PANalytical X'Pert3 Pro [31,32,37]. The average size of crystallites was calculated using the Scherrer's formula (1)

$$G = k\lambda/\beta\cos\theta \quad (1)$$

Where G = crystallite size (nm), k = equipment constant (0.5), λ = radiation wavelength, β = full-width at half maximum, and θ = Bragg angle [37,38].

The particle size distribution (PSD) analysis powder THC was done with the help of Malvern Mastersizer 3000 (UK) using the wet method. Ultraviolet-visible spectroscopy (UV-Vis) analysis was carried out using Shimadzu UV-2400PC, Japan. Fourier transform infrared (FT-IR) spectroscopy of THC was performed on Spectrum ES (Perkin Elmer, USA) FT-IR spectrometer. Likewise, the differential scanning calorimetry (DSC) analysis of THC was performed with the help of DSC Q200, TA instruments. The thermal gravimetric analysis (TGA) thermograms of THC were performed with the help of TGA Q50 TA instruments [31,32,37].

The % change in the above parameters of the Biofield Energy Treated THC was calculated compared to the control sample using equation 2:

$$\% \text{ Change} = [(\text{Treated} - \text{Control}) / \text{Control}] \times 100 \quad (2)$$

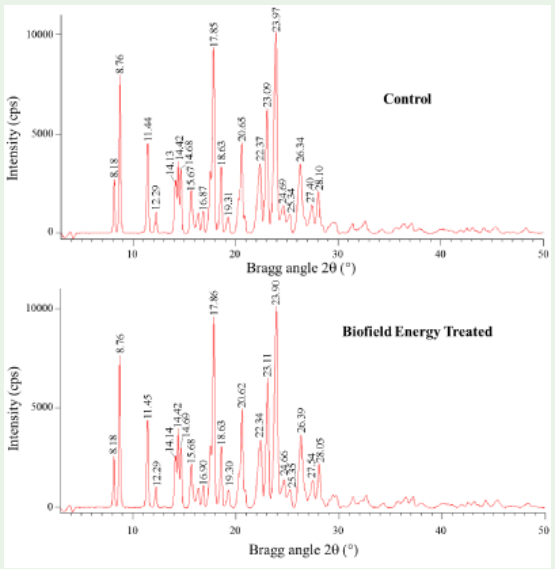

Figure 2: PXRD diffractograms of the control and treated tetrahydrocurcumin

Table 1: PXRD data for the control and treated tetrahydrocurcumin.

Entry No.	Bragg angle (°2θ)	Relative Intensity (%)			Crystallite size (G, nm)		
		Control	Treated	% Change*	Control	Treated	% Change*
1	8.2	27.47	26.07	-5.1	34.5	28.75	-16.68
2	8.8	80.2	76.4	-4.74	31.37	31.37	0
3	11.5	46.7	45.05	-3.53	20.34	21.61	6.25
4	12.3	9.95	9.77	-1.81	23.07	20.35	-11.77
5	14.1	27.79	27.25	-1.94	28.89	31.52	9.1
6	14.4	37.74	41.04	8.74	43.37	38.55	-11.12
7	14.7	33.82	30.64	-9.4	24.78	23.13	-6.67
8	15.7	22.87	22.77	-0.44	24.81	24.81	0
9	16.4	10.33	9.44	-8.62	31.61	23.17	-26.68
10	16.9	11.17	9.83	-12	28.99	28.99	0
11	17.5	32.83	32.47	-1.1	29.01	31.65	9.1
12	17.9	98.83	100	1.18	21.77	23.22	6.67
13	18.6	32.38	29.65	-8.43	26.82	23.24	-13.34
14	19.3	8.01	9.07	13.23	24.93	26.85	7.7
15	20.3	17.47	17.47	0	38.85	31.78	-18.19
16	20.7	43.31	50.76	17.2	20.57	24.98	21.43
17	20.9	8.19	8.46	3.3	31.81	26.92	-15.39
18	22.4	31.15	31.4	0.8	49.86	49.85	-0.01
19	23.1	65.49	65.01	-0.73	23.41	23.41	0
20	23.9	100	91.9	-8.1	11.72	49.99	326.39
21	24.7	14.55	14.54	-0.07	20.72	23.48	13.33
22	25.4	8.4	7.52	-10.48	23.51	22.04	-6.25
23	26.4	36.4	33.57	-7.77	18.6	22.09	18.72
24	27.5	14.75	12.13	-17.76	23.61	25.31	7.18
25	28.1	21.51	22.82	6.09	22.17	23.64	6.66

*denotes the percentage change in the peak intensities/crystallite size of the treated sample compared with the control sample.

Results and Discussion

Powder X-ray Diffraction (PXRD) Analysis

The sharp and intense peaks in PXRD diffractograms of the control and Biofield Energy Treated tetrahydrocurcumin (Figure 2) indicating that both the samples were crystalline in nature. The crystallites size were calculated with the help of Scherrer equation [37,38].

The PXRD diffractogram of the control and Biofield Energy Treated THC showed highest peak intensity (100%) at Bragg's angle (2θ) equal to 23.97° and 17.86° (Table 1, entry 20 and 12), respectively. Besides this, the relative intensities of the other XRD peaks (Table 1) also significantly altered in the Biofield Energy Treated sample compared to the control sample. The overall relative peak intensities of the in the Biofield Energy Treated sample were significantly altered ranging from -17.76% to 17.20% compared to the control sample. Similarly, the overall crystallite size of the treated sample was altered ranging from -26.68% to 326.39% compared to the control sample. Overall, the average particle size of the Biofield Energy Treated sample was reduced by 2.50% compared to the control sample.

The relative peak intensity of each diffraction face of the crystalline compound changes according to the crystal morphology [39], and alterations in the XRD pattern provide the proof of polymorphic transitions [40,41]. Changes in the crystallite size and relative peak intensities revealed that the crystal sizes of the Biofield Energy Treated THC was decreased from the control sample. Thus, it can be anticipated that the decreased in the crystallite size and relative peak intensities of the THC were due to the energy transferred through the Trivedi Effect®-Biofield Energy Healing Treatment and this probably introduced a new polymorphic form of THC. Polymorphic forms of pharmaceuticals have the significant effects on the drug performance, such as bioavailability, therapeutic efficacy, and toxicity, because their thermodynamic and physicochemical properties like melting point, energy, stability, and especially solubility, are different from the original [42,43]. Thus, it can be anticipated that Mr. Trivedi's Biofield

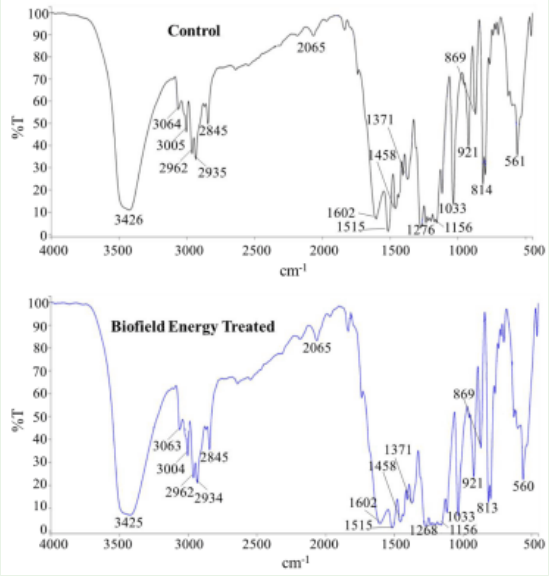

Figure 3: FT-IR spectra of the control and treated THC.

Energy Treatment (the Trivedi Effect®) could be a very useful method for the production of novel crystal polymorph of THC that might improve the bioavailability and its therapeutic performance.

Particle Size Distribution (PSD) Analysis

Particle size values of the control and Biofield Energy Treated THC were investigated, and the results are presented in Table 2. The particle size values in the Biofield Energy Treated sample was a significantly decreased by 11.58% (d_{10}), 14.41% (d_{50}), 15.53% (d_{90}), and 15.23% {D(4,3)} compared to the control sample. The surface area of the Biofield Energy Treated sample was significantly increased by 14.24% compared with the control THC.

Table 2: Particle size values and surface area of the control and treated

Parameter	d_{10} (µm)	d_{50} (µm)	d_{90} (µm)	D(4,3) (µm)	Surface area (m^2/g)
Control	19	58.3	206	88	171.4
Biofield Energy Treated	16.8	49.9	174	74.6	195.8
% Change*	-11.58	-14.41	-15.53	-15.23	14.24

*denotes the percentage change in the particle size values and surface area of the treated sample with respect to the control sample.

The particle size and surface area of the pharmaceuticals play a vital role in the solubility, absorption, dissolution, and bioavailability [44-46]. Smaller the particle size and higher surface area enhance the solubility of the solid particles as well as increase the dissolution rate and bioavailability [46,47]. Thus, it is anticipated that the Trivedi Effect®-Consciousness Energy Healing Treated THC might be absorbed in a faster rate from the gut and thus, can offer better bioavailability than the untreated sample.

Fourier Transform Infrared (FT-IR) Spectroscopy

The FT-IR spectra of the control and Biofield Energy Treated THC showed the clear stretching and bending peak in the functional group and fingerprint region (Figure 3). The broad peaks in the functional group region of both the spectra were observed near 3425 cm^{-1} due to O-H stretching. Aromatic C-H stretching at 3004 cm^{-1} and aliphatic C-H stretching at 2962 cm^{-1}, 2934 cm^{-1}, and 2845 cm^{-1} were observed in both the samples. An intense peak at 1602 cm^{-1} was due to the C=O stretching of the diketo functional group in both the control and Biofield Energy Treated THC (Figure 3). The spectra of both the samples exhibited the sharp, prominent vibrational bands at 1165 cm^{-1} and 1033 cm^{-1} due to the C-O (Ar-OH) and OCH_3 (Ar-O-R) stretching. The experimental FT-IR data of the control and Biofield Energy Treated samples were matched with the literature reported values of THC [48]. The fingerprint region of both the samples remained same. The FT-IR spectra did not display any significant alteration in the vibrational frequencies. Overall results suggested that there was no significant alteration in the structural properties of the Biofield Energy Treated sample compared to the control sample.

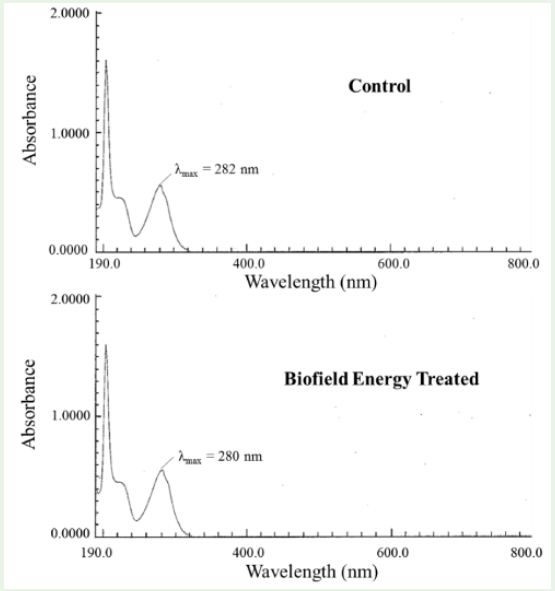

Figure 4: UV-Vis spectra of the control and treated THC.

Ultraviolet-Visible Spectroscopy (UV-Vis) Analysis

The UV-visible spectra of the control and treated THC are shown in Figure 4. The UV-V is spectrum of the control sample showed the maximum absorbance (λ_{max}) at 282 nm, whereas the Biofield Energy Treated sample exhibited the maximum absorbance at 280 nm. According to the literature, the λ_{max} for THC is 280 nm [49]. The peak at 282 nm in control and 280 nm in the Biofield Energy Treated THC showed a minor shift of absorbance maxima from 0.5511 to 0.5499.

Table 3: DSC data for both the control and treated samples of THC.

Description	1st Peak		2nd Peak	
	T_{peak} (°C)	ΔH_{fusion} (J/g)	T_{peak} (°C)	ΔH_{fusion} (J/g)
Control sample	92.98	98.92	352.33	158.4
Biofield Energy Treated sample	92.61	98.85	348.37	108
% Change*	-0.4	-0.07	-1.12	-31.82

T_{peak}: Peak melting temperature, **ΔH:** Latent heat of fusion, *denotes the percentage change of the treated sample with respect to the control sample.

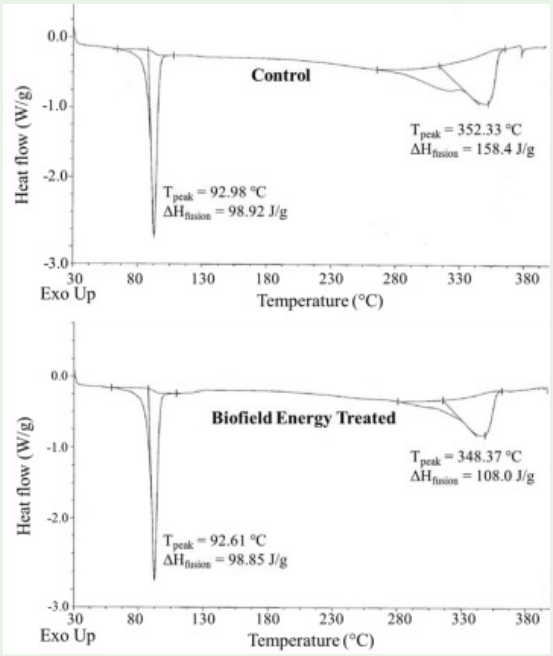

Figure 5: DSC thermograms of the control and treated THC.

Differential Scanning Calorimetry (DSC) Analysis

The DSC thermograms of the control and Biofield Energy Treated THC exhibited the sharp endothermic inflection at 92.98 and 92.61°C, respectively, which was due to the melting temperature of THC (Figure 5). The results suggested that the melting temperature of the treated THC was very close and slightly decreased compared to the control THC (Table 3). The result showed no significant alteration

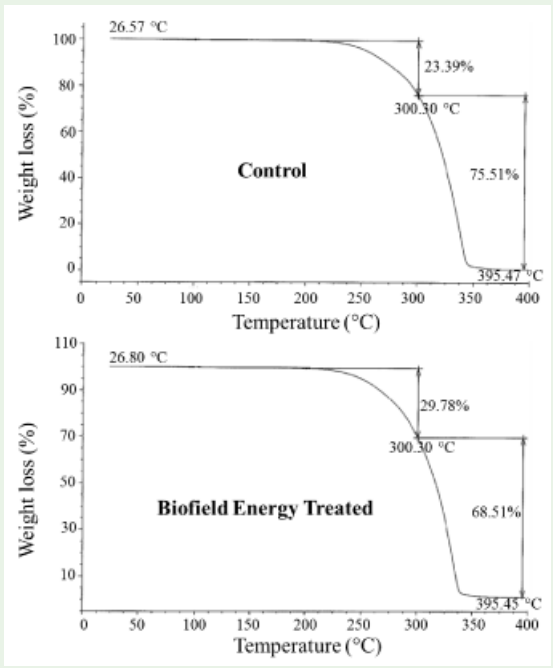

Figure 6: TGA thermograms of the control and treated THC.

Table 4: Thermal degradation steps of the control and treated samples of THC

Step	TGA (% Weight loss)			DTG (T_{max})		
	Control	Treated	% Change*	Control	Treated	% Change*
1st step of degradation	23.39	29.78	27.32	337.81	332.62	-1.54
2nd step of degradation	75.51	68.51	-9.27			
Total weight loss	98.9	98.29	-0.62			

T_{max}: maximum thermal degradation temperature; *denotes the % change of the treated sample compared with the control sample.

in the latent heat of fusion (ΔH) in the Biofield Energy Treated (98.85 J/g) THC compared to the control sample (98.92J/g) (Table 3). The 2nd broad endothermic peak in the control and Biofield Energy Treated samples may be due to the slow degradation of non-volatile intermediates according to the literature [50]. The degradation temperature and ΔH of the Biofield Energy Treated sample (2nd peak) were decreased by 1.12% and 31.82%, respectively compared to the control sample. The DSC data indicated the decrease in the thermal stability of THC after the Biofield Energy Treatment.

Thermal Gravimetric Analysis (TGA)

The TGA thermograms of the control and treated samples exhibited two steps of thermal degradation (Figure 6). The percentage weight loss in the Biofield Energy Treated THC was significantly increased by 27.32% in the 1st step of degradation, while the percentage weight loss in the 2nd step of degradation was reduced by 9.27% compared with the control sample (Table 4). The overall weight loss in the Biofield Energy Treated THC was decreased by 0.62% compared with the control sample.

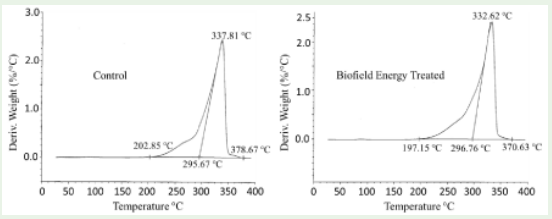

Figure 7: DTG thermograms of the control and treated THC.

The DTG thermograms of the control and Biofield Energy Treated THC (Figure 7) disclosed maximum thermal degradation temperature (T_{max}) at 337.81°C and 332.62 °C, respectively. The decomposition temperature of the Biofield Energy Treated THC was slightly decreased by 1.54% compared to the control sample (Table 4).

Overall, the thermal analysis revealed that the thermal stability of the Biofield Energy Treated THC was decreased compared to the control sample. Reduced thermodynamic stability favours the enhancement of the dissolution rate and bioavailability of the pharmaceutical compound [51]. This indicated that the solubility, dissolution, and bioavailability of the treated sample might have increased compared to the control sample.

Conclusions

The Trivedi Effect®-Consciousness Energy Healing Treatment showed a significant impact on the physicochemical, thermal, and behavioral properties of THC. The PXRD data of the control and Biofield Energy Treated samples showed that the THC was crystalline in nature. The relative peak intensities and crystallite sizes of the Biofield Energy Treated sample were significantly altered from -17.76% to 17.20% and from -26.68% to 326.39%, respectively compared to the control sample. However, the average crystallite size of the treated THC was decreased by 2.50% compared to the control sample. The particle size of the treated sample at d_{10}, d_{50}, d_{90}, and D(4,3) values were significantly decreased by 11.58%, 14.41%, 15.53%, and 15.23, respectively compared with the control sample. Simultaneously, the surface area of the treated sample was significantly increased by 14.24% compared with the control sample. The melting point and latent heat of fusion were decreased in the treated sample compared to the control sample. The TGA thermograms of both the samples exhibited two steps of thermal degradation and the weight loss in the Biofield Energy Treated THC was decreased compared with the control sample. Overall thermal analysis indicated that the thermal stability of the Biofield Energy Treated THC was declined compared with the control sample. Thus, Energy of Consciousness Healing Treatment might lead to produce a new polymorphic form of THC, which would be more soluble and bioavailable compared with the untreated THC. The Biofield Energy Treated THC would be very useful to design better nutraceutical and pharmaceutical formulations which might offer better therapeutic response against various inflammatory diseases, arthritis, cancer, diabetes, hepatotoxicity, nephrotoxicity, the ageing process, psoriasis, scleroderma atherosclerotic lesions treatment, tumors of skin, colon, pancreas, and breast.

Acknowledgements

The authors are grateful to GVK Biosciences Pvt. Ltd., Trivedi Science, Trivedi Global, Inc., and Trivedi Master Wellness for their assistance and support during this work.

References

1. GM Holder, JL Plummer, AJ Ryan. Metabolism and excretion of curcumin (1,7-bis-(4-hydroxy-3-methoxyphenyl)-1,6-heptadiene-3,5-dione) in the rat. Xenobiotica. 1978; 8: 761-768.
2. Aggarwal BB, Deb L, Prasad S. Curcumin differs from tetrahydrocurcumin for molecular targets, signaling pathways and cellular responses. Molecules. 2014; 20: 185-205.
3. Lai CS, Wu JC, Yu SF, Badmaev V, Nagabhushanam K, Ho CT, et al. Tetrahydrocurcumin is more effective than curcumin in preventing azoxymethane-induced colon carcinogenesis. Mol Nutr Food Res. 2011; 55: 1819-1828.
4. Yoysungnoen P, Wirachwong P, Changtam C, Suksamrarn A, Patumraj S. Anti-cancer and anti-angiogenic effects of curcumin and tetrahydrocurcumin on implanted hepatocellular carcinoma in nude mice. World J Gastroenterol. 2008; 7: 14: 2003-2009.
5. Park S, Lee LR, Seo JH, Kang S. Curcumin and tetrahydrocurcumin both prevent osteoarthritis symptoms and decrease the expressions of pro-inflammatory cytokines in estrogen-deficient rats. Genes Nutr. 2016; 11: 2.
6. Naito M, Wu X, Normura H, Kodama M, Kato Y, Kato Y, et al. The protective effect of tetrahydrocurcumin on oxidative stress in cholesterol-fed rabbits. J Atheroscler Thromb. 2002; 9: 243-250.
7. Wu JC, Tsai ML, Lai CS, Wang YJ, Ho CT, Pan H. Chemopreventative effects of tetrahydrocurcumin on human diseases. Food Funct. 2014; 5: 12-27.
8. Girija CR, Begum NS, Syed AA, Thiruvenkatam V. Hydrogen-bonding and C-H...[π] interactions in 1,7-bis(4-hydroxy-3-methoxyphenyl)heptane-3,5-dione (tetrahydrocurcumin). Acta Crystallographica Section C: Crystal Structure Communications. 2004; 60: o611-o613.
9. Neyrinck AM, Alligier M, Memvanga PB, Nevraumont E, Larondelle Y, Préat V, et al. Curcuma longa extract associated with white pepper lessens high fat diet-induced inflammation in subcutaneous adipose tissue. PLoS One. 2013; 8: e81252.
10. Trivedi MK, Tallapragada RM, Branton A, Trivedi D, Nayak G, Latiyal O, et al. Potential impact of biofield treatment on atomic and physical characteristics of magnesium. Vitam Miner. 2015; 3: 129.
11. Trivedi MK, Tallapragada RM, Branton A, Trivedi D, Nayak G, Latiyal O, et al. Physicochemical characterization of biofield energy treated calcium carbonate powder. Am J Health Res. 2015; 3: 368-375.
12. Rubik B. The biofield hypothesis: Its biophysical basis and role in medicine. J Altern Complement Med. 2002; 8: 703-717.
13. Nemeth L. Energy and biofield therapies in practice. Beginnings. 2008; 28: 4-5.
14. Rivera-Ruiz M, Cajavilca C, Varon J. Einthoven's string galvanometer: The first electrocardiograph. Tex Heart Inst J. 2008; 35: 174-178.
15. Koithan M. Introducing complementary and alternative therapies. J Nurse Pract. 2009; 5: 18-20.
16. Trivedi MK, Tallapragada RM, Branton A, Trivedi D, Nayak G, Latiyal O, et al. Characterization of physical and structural properties of aluminum carbide powder: Impact of biofield treatment. J Aeronaut Aerospace Eng. 2015; 4: 142.
17. Trivedi MK, Nayak G, Patil S, Tallapragada RM, Latiyal O, Jana S. Impact of biofield treatment on atomic and structural characteristics of barium titanate powder. Ind Eng Manage. 2015; 4: 166.
18. Trivedi MK, Patil S, Nayak G, Jana S, Latiyal O. Influence of biofield treatment on physical, structural and spectral properties of boron nitride. J Material Sci Eng. 2015; 4: 181.
19. Trivedi MK, Nayak G, Patil S, Tallapragada RM, Latiyal O, Jana S. Characterization of physical and structural properties of brass powder after biofield treatment. J Powder Metall Min. 2015; 4: 134.
20. Trivedi MK, Branton A, Trivedi D, Nayak G, Mondal SC. Morphological characterization, quality, yield and DNA fingerprinting of biofield energy treated alphonso mango (*Mangifera indica L.*). J Food Nutr Sci. 2015; 3: 245-250.
21. Trivedi MK, Branton A, Trivedi D, Nayak G, Mondal SC, et al. Evaluation of plant growth, yield and yield attributes of biofield energy treated mustard (*Brassica juncea*) and chick pea (*Cicer arietinum*) seeds. Agriculture, Forestry and Fisheries. 2015; 4: 291-295.
22. Trivedi MK, Branton A, Trivedi D, Nayak G, Mondal SC. Evaluation of plant growth regulator, immunity and DNA fingerprinting of biofield energy treated mustard seeds (*Brassica juncea*). Agriculture, Forestry and Fisheries. 2015; 4: 269-274.
23. Trivedi MK, Patil S, Shettigar H, Mondal SC, Jana S. The potential impact of biofield treatment on human brain tumor cells: A time-lapse video microscopy. J Integr Oncol. 2015; 4: 141.
24. Trivedi MK, Patil S, Shettigar H, Gangwar M, Jana S. In vitro evaluation of biofield treatment on cancer biomarkers involved in endometrial and prostate cancer cell lines. J Cancer Sci Ther. 2015; 7: 253-257.
25. Trivedi MK, Patil S, Shettigar H, Mondal SC, Jana S. *In vitro* evaluation of biofield treatment on *Enterobacter cloacae*: Impact on antimicrobial susceptibility and biotype. J Bacteriol Parasitol. 2015; 6: 241.
26. Trivedi MK, Patil S, Shettigar H, Mondal SC, Jana S. Evaluation of biofield modality on viral load of Hepatitis B and C Viruses. J Antivir Antiretrovir. 2015; 7: 083-088.
27. Trivedi MK, Patil S, Shettigar H, Mondal SC, Jana S. An impact of biofield treatment: Antimycobacterial susceptibility potential using BACTEC 460/MGIT-TB System. Mycobact Dis. 2015; 5: 189.

28. Trivedi MK, Branton A, Trivedi D, Nayak G, Mondal SC, Jana S. Antimicrobial sensitivity, biochemical characteristics and biotyping of *Staphylococcus saprophyticus*: An impact of biofield energy treatment. J Women's Health Care. 2015; 4: 271.

29. Trivedi MK, Branton A, Trivedi D, Nayak G, Mondal SC, Jana S. Evaluation of antibiogram, genotype and phylogenetic analysis of biofield treated *Nocardia otitidis*. Biol Syst Open Access. 2015; 4: 143.

30. Trivedi MK, Branton A, Trivedi D, Nayak G, Charan S, Jana S. Phenotyping and 16S rDNA analysis after biofield treatment on *Citrobacter braakii*: A urinary pathogen. J Clin Med Genom. 2015; 3: 129.

31. Trivedi MK, Branton A, Trivedi D, Nayak G, Wellborn BD, Jana S. Characterization of physicochemical, thermal, structural, and behavioral properties of magnesium gluconate after treatment with the Energy of Consciousness. Int J Pharmacy Chem. 2017; 3: 1-12.

32. Trivedi MK, Branton A, Trivedi D, Nayak G, Nykvist CD, Jana S. Evaluation of the physicochemical, spectral, and thermal properties of sodium selenate treated with the Energy of Consciousness (the Trivedi Effect®). Adv Biosci Bioeng. 2017; 5: 12-21.

33. Trivedi MK, Patil S, Shettigar H, Bairwa K, Jana S. Effect of biofield treatment on spectral properties of paracetamol and piroxicam. Chem Sci J. 2015; 6: 98.

34. Trivedi MK, Branton A, Trivedi D, Shettigar H, Bairwa K, Jana S. Fourier transform infrared and ultraviolet-visible spectroscopic characterization of biofield treated salicylic acid and sparfloxacin. Nat Prod Chem Res. 2015; 3: 186.

35. Chereson R. Bioavailability, bioequivalence, and drug selection. In: Makoid CM, Vuchetich PJ, Banakar UV (Eds) Basic pharmacokinetics (1st Edn) Pharmaceutical Press, London. 2009.

36. Trivedi MK, Mohan TRR. Biofield energy signals, energy transmission and neutrinos. American Journal of Modern Physics. 2016; 5: 172-176.

37. Trivedi MK, Sethi KK, Panda P, Jana S. Physicochemical, thermal and spectroscopic characterization of sodium selenate using XRD, PSD, DSC, TGA/DTG, UV-vis, and FT-IR. Marmara Pharm J. 2017; 21: 311-318.

38. Langford JI, Wilson AJC. Scherrer after sixty years: A survey and some new results in the determination of crystallite size. J Appl Cryst. 1978; 11: 102-113.

39. Inoue M, Hirasawa I. The relationship between crystal morphology and XRD peak intensity on $CaSO_4.2H_2O$. J Crystal Growth. 2013; 380: 169-175.

40. Raza K, Kumar P, Ratan S, Malik R, Arora S. Polymorphism: The phenomenon affecting the performance of drugs. SOJ Pharm Pharm Sci. 2014; 1: 10.

41. Brittain HG. Polymorphism in pharmaceutical solids in Drugs and Pharmaceutical Sciences, volume 192, 2nd Edn, Informa Healthcare USA, Inc., New York. 2009.

42. Censi R, Martino PD. Polymorph Impact on the Bioavailability and Stability of Poorly Soluble Drugs. Molecules. 2015; 20: 18759-18776.

43. Blagden N, de Matas M, Gavan PT, York P. Crystal engineering of active pharmaceutical ingredients to improve solubility and dissolution rates. Adv Drug Deliv Rev. 2007; 59: 617-630.

44. Chereson R. Bioavailability, bioequivalence, and drug selection. In: Makoid CM, Vuchetich PJ, Banakar UV (Eds) Basic pharmacokinetics (1st Edn) Pharmaceutical Press, London. 2009.

45. Khadka P, Ro J, Kim H, Kim I, Kim JT, Kim H, et al. Pharmaceutical particle technologies: An approach to improve drug solubility, dissolution and bioavailability. Asian J Pharm Sci. 2014; 9: 304-316.

46. Mosharrof M, Nyström C. The effect of particle size and shape on the surface specific dissolution rate of microsized practically insoluble drugs. Int J Pharm. 1995; 122: 35-47.

47. Buckton G, Beezer AE. The relationship between particle size and solubility. Int J Pharmaceutics. 1992; 82: R7-R10.

48. Limtrakul P, Chearwae W, Shukla S, Phisalphong C, Ambudkar SV. Modulation of function of three ABC drug transporters, P-glycoprotein (ABCB1), mitoxantrone resistance protein (ABCG2) and multidrug resistance protein 1 (ABCC1) by tetrahydrocurcumin, a major metabolite of curcumin. Mol Cell Biochem. 2007; 296: 85-95.

49. Heath DD, Pruitt MA, Brenner DE, Begum AN, Frautschy SA, Rock CL. Tetrahydrocurcumin in plasma and urine: Quantitation by high performance liquid chromatography. J Chromatogr B. 2005; 824: 206-212.

50. Jasim F, Talib T. Some observations on the thermal behavior of curcumin under air and argon atmospheres. J Thermal Analysis. 1992; 38: 2549-2552.

51. Zhao Z, Xie M, Li Y, Chen A, Li G, Zhang J, et al. Formation of curcumin nanoparticles via solution-enhanced dispersion by supercritical CO_2. Int J Nanomedicine. 2015; 10: 3171-3181.